

magnetized plasma is convected either toward or away from Jupiter by the reconnection process. The angular velocity of the plasma initially increases inward of the reconnection point, producing a corotation lead. Outward from this point, it decreases and the field is swept backward out of the meridian plane. This backward sweep of the field began before the sudden northward turning on 14 June and lasted about 4 min. Then, the field reverted to the usual anticorrelated radial and azimuthal fields characteristic of quiet times. The 17 June event has the anticorrelated radial and azimuthal fields for the entire period of enhanced vertical field.

On short time scales when the reconnection rate is high, the inertia of the mass of the thicker part of the current sheet represents an obstacle to the reconnected plasma. The newly reconnected magnetized plasma piles up against the current sheet and creates a thick region of plasma surrounding it. Evidence for the thickening can be seen in the noise and weakened radial field in the smaller event. The noise and weakened radial field are signs of hot plasma far from the center of the current sheet ( $\sim 7 R_J$ ), as estimated from a model (8).

The vertical transients in the magnetic field (Fig. 2) occurred throughout June 1997 when Galileo was at local times greater than 00:40 and radial distances  $>50 R_J$ , but few were as strong as our two examples. Similar behavior is seen in the shorter segments of data on other Galileo orbits in the region postmidnight (before 3 AM local time) and  $>50 R_J$  from the planet. These orbits also contain energetic particle bursts possibly associated with a reconfiguration of the magnetic field (9). Voyager 2 was the only previous mission to pass through this region and did not observe such magnetic events (3). The absence of similar magnetic signatures in the Voyager 2 data may relate to its greater radial velocity so that Voyager spent much less time in the active region.

It is difficult with a single satellite to determine the size of the affected region, especially in the radial direction. The disturbed vertical field lasted about 30 min, during which time the planet rotated about  $20^\circ$ . The arc of rotating plasma that moves past Galileo in 30 min at these distances is about  $25 R_J$  if the plasma is nearly corotating. We would expect that the radial extent might be similar. Thus, these disturbances appear to be large but not global events and may represent only a fraction of the reconnection taking place in the magnetodisk (10). The rapidity of the onset is not surprising given that the reconnection should accelerate the plasma to the order of the Alfvén velocity that may be higher than 5000 km/s in the tail lobes. Thus, a radial

displacement of  $12.5 R_J$  might occur in a time as short as 3 min, not inconsistent with the onsets of our two observed events.

## REFERENCES AND NOTES

1. M. G. Kivelson, K. K. Khurana, J. D. Means, C. T. Russell, R. C. Snare, *Space Sci. Rev.* **60**, 357 (1992).
2. E. J. Smith, L. Davis Jr., D. E. Jones, in *Jupiter*, T. Gehrels, Ed. (Univ. of Arizona Press, Tucson, AZ, 1979), pp. 788–920.
3. M. Acuña, K. W. Behannon, J. E. P. Connerney, in *Physics of the Jovian Magnetosphere*, A. J. Dessler, Ed. (Cambridge Univ. Press, London, 1983), pp. 1–50.
4. A. Balogh *et al.*, *Science* **257**, 1515 (1992).
5. V. M. Vasyliunas, in (3), pp. 395–453.
6. T. W. Hill, A. J. Dessler, C. K. Goertz, *ibid.*, pp. 353–394.
7. C. T. Russell and R. M. McPherron, *Space Sci. Rev.* **15**, 205 (1973).
8. K. K. Khurana, *J. Geophys. Res.* **102**, 11295 (1997).
9. N. Krupp *et al.*, *Eos (Fall Suppl.)* **78** (no. 46), F470 (1997).
10. Similar to the two neutral points in Earth's tail, one close and transitory and the other distant and more permanent, there may exist a more steady-state neutral line at a greater radial distance in the jovian tail (5).
11. D. E. Huddleston, C. T. Russell, M. G. Kivelson, K. K. Khurana, L. Bennett, *J. Geophys. Res.*, in press.
12. Supported by NASA through the Jet Propulsion Laboratory.

29 December 1997; accepted 24 March 1998

# Ferromagnetism in LaFeO<sub>3</sub>-LaCrO<sub>3</sub> Superlattices

Kenji Ueda, Hitoshi Tabata, Tomoji Kawai\*

Ferromagnetic spin order has been realized in the LaCrO<sub>3</sub>-LaFeO<sub>3</sub> superlattices. Ferromagnetic coupling between Fe<sup>3+</sup> and Cr<sup>3+</sup> through oxygen has long been expected on the basis of Anderson, Goodenough, and Kanamori rules. Despite many studies of Fe-O-Cr-based compounds, random positioning of Fe<sup>3+</sup> and Cr<sup>3+</sup> ions has frustrated the observation of ferromagnetic properties. By creating artificial superlattices of Fe<sup>3+</sup> and Cr<sup>3+</sup> layer along the [111] direction, ferromagnetic ordering has been achieved.

A magnetic interaction between two magnetic ions through a nonmagnetic ion (such as oxygen) was first proposed by Kramers (1) and was systematized by Anderson (2). Later, this so-called superexchange interaction was refined by Goodenough (3) and Kanamori (4) at a level so that this theory can be applied to various magnetic materials. According to their rules, we can estimate and predict whether a magnetic interaction through a superexchange interaction between two spins has a ferromagnetic (FM) or antiferromagnetic (AF) character. Many researchers have used this idea as a starting point for synthesizing ferromagnets. On the basis of these rules, the 180° superexchange interaction in a metal dimer bridged via oxygen that has a  $d^3-d^5$  electron state ( $\angle M-O-M = 180^\circ$  and  $M = Fe^{3+}$ ,  $Cr^{3+}$ , and so forth) is predicted to have FM order (4). The most typical and still unachieved combination is Fe-O-Cr systems (5). It is expected that if Fe<sup>3+</sup> and Cr<sup>3+</sup> ions are introduced alternately in the B site of perovskite-type transition metal oxides (ABO<sub>3</sub>), the synthesis of FM materials can be achieved. Although some attempts to synthesize such materials have been made by sintering methods, the atomic order of

Fe-O-Cr has not been achieved because such materials phase separate into Fe oxide and Cr oxide phases (6). As a result, a FM ordered phase has not been obtained, and the materials have been shown to have an AF character (7, 8).

The single-phase LaCrO<sub>3</sub> and LaFeO<sub>3</sub> have AF structures with both inter- and intralayer antiparallel spin alignments and Neel temperatures ( $T_N$ ) of 280 and 750K, respectively (9–11). If an artificial superlattice of LaCrO<sub>3</sub>-LaFeO<sub>3</sub> is synthesized by depositing alternating layers of LaCrO<sub>3</sub> and LaFeO<sub>3</sub> along the [111] direction, it may be possible to form films that have various magnetic properties by controlling the stacking periodicity. Ferromagnetism can occur especially in the case of one layer by one layer stacking on the (111) surface because Fe<sup>3+</sup> and Cr<sup>3+</sup> ions are bridged by oxygen ions alternately in the film (Fig. 1).

We have synthesized a FM artificial superlattice by alternately stacking one unit layer of LaCrO<sub>3</sub> and LaFeO<sub>3</sub> on a SrTiO<sub>3</sub> [111] single crystal by laser molecular beam epitaxy (MBE) (Fig. 1). Such materials cannot be obtained in the conventional bulk phase because they are thermodynamically unstable (6–8). Furthermore, even if phase separation is avoided so that Fe<sup>3+</sup> and Cr<sup>3+</sup> ions mix randomly, AF interactions are dominant in the material because the Fe<sup>3+</sup>-O-Cr<sup>3+</sup> ordered phase could not be

The Institute of Scientific and Industrial Research, Osaka University, 8-1 Mihogaoka, Ibaraki, Osaka 567, Japan.

\*To whom correspondence should be addressed.

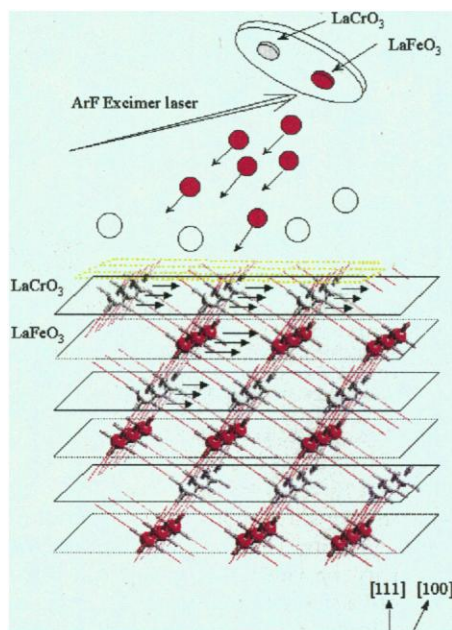


**Fig. 1.** A schematic diagram for the construction of the  $\text{LaCrO}_3$ - $\text{LaFeO}_3$  superlattice along the [111] direction by laser molecular beam epitaxy. The CrO layer and FeO layer are stacked alternately. For clarity the atoms of oxygen and lanthanum have been omitted.

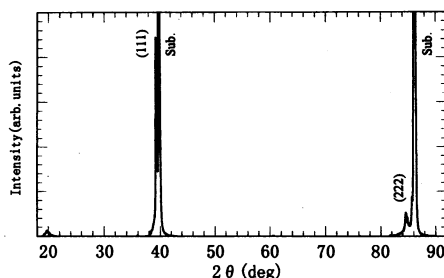
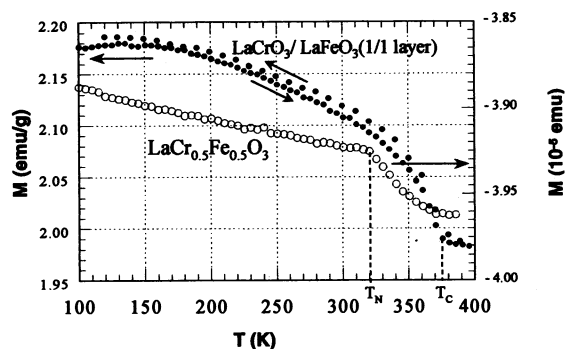


**Fig. 2.** X-ray diffraction pattern of the  $\text{LaCrO}_3$ - $\text{LaFeO}_3$  (1/1 layer) superlattice formed on a  $\text{SrTiO}_3$  (111) substrate.

achieved statistically. An artificial superlattice is a powerful tool for synthesizing these materials (12).

The magnetic superlattices were constructed as follows. The  $\text{LaCrO}_3$  and  $\text{LaFeO}_3$  layers were stacked by multiple target pulsed laser deposition (PLD) (Fig. 1). An ArF excimer laser pulse was focused on the targets to induce ablation, and the ablated atoms and ions were deposited on the  $\text{SrTiO}_3$  (111) substrate. Atomic-scale control of the crystal growth could be achieved by combining the PLD method with reflection-high-energy electron diffraction (RHEED) observations (12, 13). The distance between the Fe and Cr layers was varied from 2.3 Å (1 unit layer) to 16.1 Å (7 unit layers), and the total thickness of the superlattices was 600 to 1100 Å (14).

X-ray diffraction measurements of La-



$\text{CrO}_3$ - $\text{LaFeO}_3$  superlattices in each stacking periodicity exhibit characteristics of artificial structures (Fig. 2). The distance between layers (corresponding to the distance between FeO-CrO layers) is 2.29 Å, and the full width at half maximum is  $\sim 0.28^\circ$  to  $0.20^\circ$ , which indicates that our sample is well constructed, as desired. The RHEED measurements of the  $\text{LaCrO}_3$ - $\text{LaFeO}_3$  artificial superlattices on  $\text{SrTiO}_3$  (111) substrate showed streaked patterns, indicating that the films were formed epitaxially and are highly crystallized up to the topmost surface.

The temperature dependence of magnetization for the  $\text{LaCrO}_3$ - $\text{LaFeO}_3$  artificial superlattices with a stacking periodicity of 1/1 layer on  $\text{SrTiO}_3$  (111) is shown in Fig. 3. In this case, a magnetic field of 1000 Oe was applied parallel to the surface of the substrate. FM transition is apparent at 375 K. The magnetization of the  $\text{LaCrO}_3$ - $\text{LaFeO}_3$  superlattices increases with decreasing temperature, and the saturation magnetization approaches  $\sim 2$  electromagnetic units/g which corresponds to about 3 Bohr magnetons ( $\mu_B$ ) at one site. From the theoretical estimation, the magnetization value of  $4 \mu_B$  per site would be expected because of the atomic order of  $\text{Fe}^{3+}(d^5)$ -O- $\text{Cr}^{3+}(d^3)$  high-spin state. Our experimental values are slightly less than the calculated one because of imperfections in the crystallinity and the atomic stacking sequence of the superlattices. The magnetization-temperature curve can be fitted with the relation

$$M/M_0 = \alpha \left( \frac{T_c - T}{T_c} \right)^\beta$$

where  $M_0$  is the saturation magnetization at  $T = 0$  and  $T_c$  is the Curie temperature. For values of  $\alpha = 1.09$  and  $\beta = 0.33$ , the curve is well reproduced. The value of  $\beta = 0.33$  is similar to that for a standard Heisenberg-type spin-spin coupling.

For artificial superlattices with larger ( $>1$  unit layer) stacking periodicity, the FM interactions are introduced in the interface between the Fe and Cr layer. Indeed, for the 7/7 layer superlattice, a FM character was

**Fig. 3.** Temperature dependence of magnetization of  $\text{LaCrO}_3$ - $\text{LaFeO}_3$  superlattice on  $\text{SrTiO}_3$  (111) (●) and that of  $\text{LaCr}_{0.5}\text{Fe}_{0.5}\text{O}_3$  solid solution film (○), measured in a 0.1-T magnetic field applied parallel to the substrate surface.

also observed and showed magnetization of  $1 \mu_B$  per site. The magnetic moment per site is obtained by assuming that the ferromagnetism comes from the interfacial layers and that other inner layers that are not directly in contact with it do not contribute a spontaneous magnetization. This is further evidence of the FM character of our superlattices.

As a reference, the  $M$ - $T$  curve of the  $\text{La}(\text{Fe}_{0.5}\text{Cr}_{0.5})\text{O}_3$  solid solution film in a 0.1-T field (Fig. 3) differs from that of the  $\text{LaCrO}_3$ - $\text{LaFeO}_3$  (1/1) superlattice. A cusp shape is observed at 320 K, which is a typical feature of antiferromagnetism. A background that increased monotonously with decreasing measured temperature was caused by the paramagnetic character of the substrate. Ferrimagnetism might also explain the  $M$ - $T$  character of the  $\text{LaCrO}_3$ -

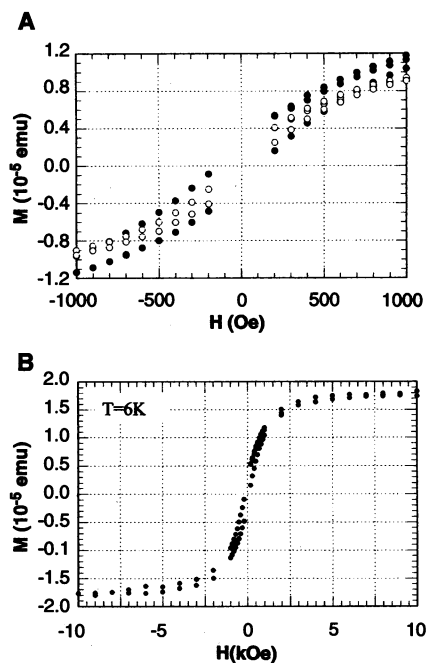


**Fig. 4.** (A) Hysteresis curves for  $\text{LaCrO}_3$ - $\text{LaFeO}_3$  on  $\text{SrTiO}_3$  (111) in the field range of  $\pm 2000$  Oe at 6 K (●) and 350 K (○). (B) Hysteresis curve at 6 K in the field range of  $\pm 10$  kOe. The magnetic field is applied parallel to the film plane.

LaFeO<sub>3</sub> (1/1) superlattice. However, the magnetization value of 3 μ<sub>B</sub> per site is too large to attribute to a ferrimagnetic order. The dependence of *M* on the magnetic field (hysteresis curve) of LaCrO<sub>3</sub>-LaFeO<sub>3</sub> artificial superlattice (1/1 sequence) on substrate (111) is shown in Fig. 4. Hysteresis was observed in the *M-H* curves in the temperature region from 6 to 350 K. The *M* is saturated under the applied field above 5 kOe (Fig. 4B). In the enlarged hysteresis curve (Fig. 4A), the remnant *M* of the superlattices decreases with increasing temperature up to 375 K. Above a *T<sub>C</sub>* of 375 K, it shows a paramagnetic character. These features are typical of FM materials. Our

results provide further evidence that the FM spin order is realized in the artificial lattice with a one by one layer stacking combination.

#### REFERENCES AND NOTES

- H. A. Kramers, *Physica* **1**, 182 (1934).
- P. W. Anderson, *Phys. Rev.* **79**, 350 (1950).
- J. B. Goodenough, *ibid.* **100**, 564 (1955).
- J. Kanamori, *J. Phys. Chem. Solids* **10**, 87 (1959).
- In the case of Ni<sup>2+</sup> and Mn<sup>4+</sup> or Co<sup>2+</sup> and Mn<sup>4+</sup>, FM ordering was reported in the bulk sample [G. Blasse, *J. Phys. Chem. Solids* **26**, 1969 (1965)].
- A. Wold and W. Croft, *J. Phys. Chem.* **63**, 447 (1959).
- A. Belayachi, M. Noguez, J.-L. Dormann, M. Taibi, *Eur. J. Solid State Inorg. Chem.* **33**, 1039 (1996).
- K. P. Belov *et al.*, *Sov. Phys. Solid State* **14**, 813 (1972).
- R. Aleorard, R. Pauthenet, J. P. Rebouillat, C. Veyret, *J. Appl. Phys.* **39**, 379 (1968).
- W. C. Koehler, E. O. Wollan, M. K. Wilkinson, *Phys. Rev.* **118**, 58 (1960).
- D. Treves, *J. Appl. Phys.* **36**, 1033 (1965).
- T. Kawai, M. Kanai, H. Tabata, *Mater. Sci. Eng.* **41**, 123 (1996).
- H. Tabata, T. Kawai, S. Kawai, *Phys. Rev. Lett.* **70**, 2633 (1993).
- Targets of LaCrO<sub>3</sub> and LaFeO<sub>3</sub> were synthesized by mixing La<sub>2</sub>O<sub>3</sub> with Cr<sub>2</sub>O<sub>3</sub>, and La<sub>2</sub>O<sub>3</sub> with α-Fe<sub>2</sub>O<sub>3</sub>, respectively, at a molar ratio of 1:1 and sintering them at 1000°C. The films were formed at 580°C in an oxygen/ozone (8%) ambient pressure of 1 mtorr. The deposition rate was 10 Å/min. All magnetic measurements were performed with a SQUID magnetometer (Quantum design MPMS-5S).

13 January 1998; accepted 23 March 1998

## Inducible Repair of Thymine Glycol Detected by an Ultrasensitive Assay for DNA Damage

X. Chris Le,\* James Z. Xing, Jane Lee, Steven A. Leadon, Michael Weinfeld\*

An ultrasensitive assay for measuring DNA base damage is described that couples immunochemical recognition with capillary electrophoresis and laser-induced fluorescence detection. The method provides a detection limit of  $3 \times 10^{-21}$  moles, an improvement of four to five orders of magnitude over current methods. Induction and repair of thymine glycols were studied in irradiated A549 cells (a human lung carcinoma cell line). Exposure of these cells to a low dose of radiation (0.25 Gray) 4 hours before a clinically relevant dose (2 Gray) enhanced removal of thymine glycols after the higher dose. These data provide evidence for an inducible repair response for radiation-induced damage to DNA bases.

DNA damage and its cellular repair are key determinants in the early stages of carcinogenesis, cancer therapy, and aging. As a result, many assays for DNA damage have been developed over the past 30 years; each has its advantages and disadvantages (1, 2). Among the important criteria to consider when assessing the usefulness of an assay are its specificity, sensitivity, and simplicity. Measurement of oxidative DNA damage generated by ionizing radiation illustrates the relative importance of each of these criteria. Ionizing radiation produces a wide assortment of DNA lesions, including a large number of base modifications, strand breaks, and DNA-protein crosslinks (3). Because of their specificity, techniques such as gas chromatography-mass spectrometry,

high-performance liquid chromatography with electrochemical and mass spectrometry detection, postlabeling, and immunoassays have proven extremely useful for analyzing modified bases (4). However, they currently lack the sensitivity required to monitor repair of the DNA of cells treated with clinically relevant doses of radiation—that is,  $\leq 2$  Gray (Gy). In addition, the first three methods involve a series of chemical derivatization or enzymatic hydrolysis and labeling steps, which means that great care must be taken to ensure that there is minimal introduction of oxidative DNA lesions by the procedure itself and that digestion and labeling reactions are optimized (5). On the other hand, electrophoretic approaches, such as pulsed-field gel electrophoresis and single-cell gel electrophoresis (the comet assay), have the capacity to detect damage at lower radiation doses but for the most part are restricted to measurement of strand breaks (6).

To monitor damage to DNA bases resulting from therapeutic doses of radiation, we have developed an assay that takes advantage of the high sensitivity (zeptomole, or  $10^{-21}$  mol) afforded by capillary electro-

phoresis coupled with laser-induced fluorescence detection (7, 8), combined with the specificity provided by monoclonal antibodies to a single lesion. Sample manipulation is limited to DNA extraction, incubation with antibodies, and capillary electrophoresis, thereby reducing potential artifacts caused by chemical or enzymatic DNA digestion. Notably, the technique requires only nanogram amounts of DNA.

To test the feasibility of the assay, we used mouse monoclonal antibodies to bromodeoxyuridine (BrdU) (9), because we could generate model DNA antigens containing a specified quantity of this modified base, and tetramethylrhodamine (TMR)-labeled secondary antibodies because of the convenient fluorescence wavelengths. To prepare the antigens, we cleaved pUC18 plasmid molecules with Sal I, filled in the overhanging termini by incorporating nucleotides including BrdU, and then ligated the plasmid molecules (10). Thus, two molecules of BrdU were incorporated per molecule of pUC18 [2690 base pairs (bp)]. Capillary electrophoresis separates the unbound secondary antibody (Fig. 1A, peak 1), the complex of secondary and primary antibody (Fig. 1B, peak 2), and the complex of antigen with the primary and secondary antibodies (Fig. 1C, peak 3). The signal in peak 3 (Fig. 1C) was produced by  $\sim 3 \times 10^{-19}$  mol of BrdU.

We compared the signals produced by BrdU-containing plasmid DNA at a concentration of 0.05 μg/ml in the absence (Fig. 1D) or presence (Fig. 1E) of unmodified pUC18 DNA (450 μg/ml), which corresponds to a final ratio of 2 BrdU molecules per  $2.42 \times 10^7$  bp. The large excess of undamaged DNA did not alter the signal in peak 3. Because the sample concentration of plasmid DNA antigen was 0.05 μg/ml and 1 nl was injected into the capillary, the signal in peak 3 represents  $\sim 6 \times 10^{-20}$  mol of BrdU. The detection limit, based on a signal-to-noise ratio of 3, was  $3 \times 10^{-21}$

X. C. Le and J. Z. Xing, Department of Public Health Sciences, Faculty of Medicine and Oral Health Sciences, University of Alberta, Edmonton, Alberta, T6G 2G3, Canada.

J. Lee and M. Weinfeld, Experimental Oncology, Cross Cancer Institute, Edmonton, Alberta, T6G 1Z2, Canada. S. A. Leadon, Department of Radiation Oncology, University of North Carolina School of Medicine, Chapel Hill, NC 27599-7512, USA.

\*To whom correspondence should be addressed. E-mail: xc.le@ualberta.ca and mweinfeld@gpu.srv.ualberta.ca